

## Evaluation of $CP$ violation in $\text{HfF}^+$

A. N. Petrov,<sup>\*</sup> L. V. Skripnikov, and A. V. Titov<sup>†</sup>

*National Research Center, Kurchatov Institute, B.P. Konstantinov Petersburg Nuclear Physics Institute, Gatchina, Leningrad District 188300, Russia*

*and Department of Physics, Saint Petersburg State University, Saint Petersburg, Petrodvoretz 198504, Russia*

V. V. Flambaum

*School of Physics, The University of New South Wales, Sydney 2052, NSW, Australia*



(Received 24 July 2018; published 8 October 2018)

$CP$  violation effects produced by the nuclear magnetic quadrupole moment (MQM), electron electric dipole moment (EDM), and scalar-pseudoscalar nucleus-electron neutral current (SP) interaction in  $^{177}\text{Hf}^{19}\text{F}^+$  and  $^{179}\text{Hf}^{19}\text{F}^+$  are calculated. The role of the hyperfine interaction is investigated. It is shown that the MQM shift can be distinguished from the electron EDM and SP ones due to the implicit dependence of the MQM shift on the hyperfine sublevel. The MQM effect is expressed in terms of the proton (EDM), QCD vacuum angle  $\theta$ , and quark chromo-EDMs.

DOI: [10.1103/PhysRevA.98.042502](https://doi.org/10.1103/PhysRevA.98.042502)

### I. INTRODUCTION

Recently, Cairncross *et al.* have obtained the limit on the electron electric dipole moment ( $e\text{EDM}$ ),  $|d_e| < 1.3 \times 10^{-28} e\text{cm}$  (90% confidence), using trapped  $^{180}\text{Hf}^{19}\text{F}^+$  ions [1] with the spinless  $^{180}\text{Hf}$  isotope. Measurements were performed on the ground rotational,  $J = 1$ , level in the metastable electronic  $H^3\Delta_1$  state. The experiment demonstrated a great potential for the investigation of time-reversal and parity-violating ( $T$ ,  $P$ -odd) effects using  $\text{HfF}^+$  ions [1,2]. In Ref. [3] it was proposed to use  $^{177}\text{Hf}^{19}\text{F}^+$  and  $^{179}\text{Hf}^{19}\text{F}^+$  ions with isotopes of hafnium which have nuclear spin  $I > 1/2$  to measure  $T$ ,  $P$ -odd effects produced by the nuclear magnetic quadrupole moment (MQM). Measurement of the nuclear MQM is promising for establishing new limits on neutron and proton EDMs, vacuum angle  $\theta$  in quantum chromodynamics, and EDMs and chromo-EDMs of quarks [4]. A corresponding experiment is discussed by Ye [5].

We have previously carried out theoretical studies of the effects induced by the nuclear MQM in  $^{229}\text{ThO}$  [4],  $^{181}\text{TaN}$  [6], and  $^{229}\text{ThF}^+$  [7] molecules. In particular, we derived analytical expressions for the energy shifts of the molecule caused by the interaction of electrons with the MQM, which can be measured in the experiment. However, the formulas do not take into account the mixing of different rotational levels by the magnetic dipole and electric quadrupole hyperfine interactions and external electric field, which change the values of the shifts.

The main goal of the present work is to perform numerical calculations of the MQM,  $e\text{EDM}$ , and scalar-pseudoscalar-nucleus-electron neutral current (SP) interaction energy shifts of different hyperfine sublevels in the ground rotational level

of  $^{177}\text{Hf}^{19}\text{F}^+$  and  $^{179}\text{Hf}^{19}\text{F}^+$  which take into account these effects.

### II. $T$ , $P$ -ODD INTERACTION HAMILTONIAN

The hafnium isotopes  $^{177}\text{Hf}$  and  $^{179}\text{Hf}$  have nuclear spin  $I^1 = 7/2$  and  $I^1 = 9/2$ , respectively. The fluorine isotope  $^{19}\text{F}$  has nuclear spin  $I^2 = 1/2$ . For the purposes of this work it is convenient to use the coupling scheme

$$\mathbf{F}_1 = \mathbf{J} + \mathbf{I}^1, \quad (1)$$

$$\mathbf{F} = \mathbf{F}_1 + \mathbf{I}^2, \quad (2)$$

where  $\mathbf{J}$  is the total molecular less nuclear spins angular momentum. The field-free energy levels of the ground rotational state with quantum number  $J = 1$  are split into three groups by the hyperfine interaction with the hafnium nucleus; they are characterized by  $F_1 = 9/2$ ,  $F_1 = 7/2$ , and  $F_1 = 5/2$  for  $^{177}\text{Hf}$  and  $F_1 = 11/2$ ,  $F_1 = 9/2$ , and  $F_1 = 7/2$  for  $^{179}\text{Hf}$  quantum numbers. The hyperfine interaction with the fluorine nucleus further splits levels with total momentum  $F = F_1 \pm 1/2$ . Note that  $F_1$  is not exact but a good quantum number since the hyperfine interaction with the fluorine nucleus is much weaker than the hyperfine interaction with the hafnium nucleus. Finally, each hyperfine level has two parity eigenstates known as the  $\Omega$  doublet. These states are equal mixtures of the  $\Omega = \pm 1$  states, where  $\Omega$  is the projection of  $\mathbf{J}$  on the internuclear  $\hat{n}$  axis.

An external electric field mixes  $\Omega$ -doublet states of opposite parity and transforms the  $\Omega$ -doublet structure of each hyperfine level to the Stark doublet structure. For a sufficiently large electric field,  $\Omega$  becomes a good quantum number, except  $m_F = 0$  levels, which are not mixed by the electric field. Here  $m_F$  is the projection of  $\mathbf{J}$  on the laboratory  $\hat{z}$  axis which coincides with the direction of the electric field. State  $J = 1$  in the  $^{180}\text{HfF}^+$  molecule with the spinless hafnium

<sup>\*</sup>alexandernp@gmail.com

<sup>†</sup><http://www.qchem.pnpi.spb.ru>

isotope becomes almost fully polarized by the electric field  $E > 4$  V/cm [8]. The molecules  $^{177}\text{Hf}^{19}\text{F}^+$  and  $^{179}\text{Hf}^{19}\text{F}^+$  require a much larger field to be polarized (see below).

The  $T$ ,  $P$ -odd electromagnetic interaction of the nuclear magnetic quadrupole moment with electrons is described by the Hamiltonian [9]

$$H_{\text{MQM}} = -\frac{M}{2I^1(2I^1 - 1)} T_{ik} \frac{3}{2r^5} \epsilon_{jli} \alpha_j r_l r_k, \quad (3)$$

where  $\epsilon_{jli}$  is the unit antisymmetric tensor,  $\alpha$  is the vector of Dirac matrices,  $\mathbf{r}$  is the displacement of the electron from the Hf nucleus,  $M$  is the Hf nuclear MQM,

$$M_{i,k} = \frac{3M}{2I(2I - 1)} T_{i,k}, \quad (4)$$

$$T_{i,k} = I_i^1 I_k^1 + I_k^1 I_i^1 - \frac{2}{3} \delta_{i,k} I^1 (I^1 + 1). \quad (5)$$

The  $e$ EDM interaction is described by the Hamiltonian

$$H_d = 2d_e \begin{pmatrix} 0 & 0 \\ 0 & \sigma \mathbf{E} \end{pmatrix}, \quad (6)$$

$\mathbf{E}$  is the inner molecular electric field, and  $\sigma$  are the Pauli matrices.

The  $T$ ,  $P$ -odd SP interaction with a characteristic dimensionless constant  $k_{\text{SP}}$  is described by the Hamiltonian [10]

$$H_{\text{SP}} = i \frac{G_F}{\sqrt{2}} Z k_{\text{SP}} \gamma_0 \gamma_5 n(\mathbf{r}), \quad (7)$$

where  $G_F$  is the Fermi-coupling constant,  $\gamma_0$  and  $\gamma_5$  are the Dirac matrices, and  $n(\mathbf{r})$  is the nuclear density normalized to unity. For simplicity the summation over different electrons is omitted in Eqs. (3), (6), and (7).

For field-free eigenstates the expectation value for the  $T$ ,  $P$ -odd operators (3), (6), and (7) is 0. For the completely polarized molecule and neglecting the interaction between different rotational,  $J$ , and hyperfine,  $F_1$ , levels, the energy shift due to the SP,  $e$ EDM, and MQM interactions are [4]

$$\delta_d = d_e E_{\text{eff}} \Omega, \quad (8)$$

$$\delta_{\text{SP}} = k_{\text{SP}} W_{\text{SP}} \Omega, \quad (9)$$

$$\delta_M(J, F_1) = (-1)^{I^1+F} C(J, F_1) M W_M \Omega, \quad (10)$$

$$C(J, F_1) = \frac{(2J+1)}{2} \frac{\begin{pmatrix} J & 2 & J \\ -\Omega & 0 & \Omega \end{pmatrix}}{\begin{pmatrix} I^1 & 2 & I^1 \\ -I^1 & 0 & I^1 \end{pmatrix}} \begin{Bmatrix} J & I^1 & F_1 \\ I^1 & J & 2 \end{Bmatrix}, \quad (11)$$

where  $(\dots)$  means elements with  $3j$  symbols and  $\{\dots\}$  with  $6j$  symbols [11],

$$E_{\text{eff}} = \left\langle \Psi_{\Delta_1} \left| \sum_i \frac{H_d(i)}{d_e} \right| \Psi_{\Delta_1} \right\rangle, \quad (12)$$

$$W_{\text{SP}} = \left\langle \Psi_{\Delta_1} \left| \sum_i \frac{H_{\text{SP}}(i)}{k_{\text{SP}}} \right| \Psi_{\Delta_1} \right\rangle, \quad (13)$$

$$W_M = \frac{3}{2} \frac{1}{\Omega} \left\langle \Psi_{\Delta_1} \left| \sum_i \left( \frac{\alpha_i \times \mathbf{r}_i}{r_i^5} \right)_{\zeta} r_{\zeta} \right| \Psi_{\Delta_1} \right\rangle, \quad (14)$$

where  $\Psi$  is the electronic wave function of the considered  $H^3 \Delta_1$  state of the  $\text{HfF}^+$  cation.

Two sublevels within a Stark doublet are connected by the time reversal  $m_F \rightarrow -m_F$ ,  $\Omega \rightarrow -\Omega$  and therefore have opposite signs for both  $m_F$  and  $\Omega$  quantum numbers and are degenerate unless the  $T$ ,  $P$ -odd interactions are not taken into account. One can see from Eqs. (8)–(10) that states with the opposite projections of  $\Omega$  have the opposite MQM,  $e$ EDM, and SP interaction energy shifts, which give rise to a splitting between the Stark doublet sublevels to be measured in the experiment. The MQM shift can be distinguished from the other two shifts by its dependence on the  $F_1$  quantum number. For a given  $F_1$  the energy shifts are independent of the  $F$  and  $m_F$  quantum numbers provided the approximations assumed above. The exception is for  $m_F = 0$  levels, which have zero shifts, as they are equal mixtures of  $\Omega = \pm 1$  states.

In the present work we take into account the interactions with the external electric field, magnetic dipole and electric quadrupole hyperfine interactions which mix different rotational ( $J$ ) and hyperfine ( $F_1$ ) levels and modify the values of the shifts given by Eqs. (8)–(10).

### III. EVALUATION OF $T$ , $P$ -ODD SHIFTS

The MQM,  $e$ EDM, and SP interaction energy shifts have been calculated as the expectation values of Hamiltonians (3), (6), and (7) with the wave functions of the  $^{177}\text{Hf}^{19}\text{F}^+$  and  $^{179}\text{Hf}^{19}\text{F}^+$  molecules. Following Refs. [12] and [13], the energy levels and wave functions of the  $^{180}\text{Hf}^{19}\text{F}^+$  ion are obtained by the numerical diagonalization of the molecular Hamiltonian ( $\hat{\mathbf{H}}_{\text{mol}}$ ) on the basis set of the electronic-rotational wave functions

$$\Psi_{\Omega} \theta_{M,\Omega}^J(\alpha, \beta) U_{I^1 M^1}^{\text{Hf}} U_{I^2 M^2}^{\text{F}}. \quad (15)$$

Here  $\Psi_{\Omega}$  is the electronic wave function,  $\theta_{M,\Omega}^J(\alpha, \beta) = \sqrt{(2J+1)/4\pi} D_{M,\Omega}^J(\alpha, \beta, \gamma = 0)$  is the rotational wave function,  $\alpha$ ,  $\beta$ , and  $\gamma$  are the Euler angles,  $U_{I^1 M^1}^{\text{Hf}}$  and  $U_{I^2 M^2}^{\text{F}}$  are the Hf and F nuclear spin wave functions,  $M$  ( $\Omega$ ) is the projection of the molecule angular momentum,  $\mathbf{J}$ , on the laboratory  $\hat{z}$  (internuclear  $\hat{n}$ ) axis, and  $M^{1,2}$  are the projections of the nuclear angular momenta on the same axis. We write the molecular Hamiltonian for the  $^{180}\text{Hf}^{19}\text{F}^+$  molecule in the form

$$\hat{\mathbf{H}}_{\text{mol}} = \hat{\mathbf{H}}_{\text{el}} + \hat{\mathbf{H}}_{\text{rot}} + \hat{\mathbf{H}}_{\text{hfs}} + \hat{\mathbf{H}}_{\text{ext}}. \quad (16)$$

Here  $\hat{\mathbf{H}}_{\text{el}}$ ,  $\hat{\mathbf{H}}_{\text{rot}}$ , and  $\hat{\mathbf{H}}_{\text{ext}}$  are the electronic Hamiltonian, rotation of the molecule, and interaction of the molecule with the external field Hamiltonians, respectively, as they are described in Ref. [14],

$$\hat{\mathbf{H}}_{\text{hfs}} = g_{\text{F}} \mu_N I^2 \sum_i \left( \frac{\alpha_i \times \mathbf{r}_{2i}}{r_{2i}^3} \right) \quad (17)$$

$$+ g_{\text{Hf}} \mu_N I^1 \sum_i \left( \frac{\alpha_i \times \mathbf{r}_{1i}}{r_{1i}^3} \right) \quad (18)$$

$$+ -e^2 \sum_q (-1)^q \hat{Q}_q^2(I^1) \sum_i \sqrt{\frac{2\pi}{5}} \frac{Y_{2q}(\theta_{1i}, \phi_{1i})}{r_{1i}^3} \quad (19)$$

is the hyperfine interaction between electrons and a nucleus,  $g_F$  and  $g_{Hf}$  are the  $^{19}\text{F}$  and  $^{177,179}\text{Hf}$  nuclear g-factors,  $\mu_N$  is the nuclear magneton,  $\mathbf{r}_{1i}$  ( $\mathbf{r}_{2i}$ ) is the radius vector for the  $i$ th electron in the coordinate system centered on the Hf(F) nucleus, and  $\hat{Q}_q^2(I^1)$  is the quadrupole moment operator for the  $^{177,179}\text{Hf}$  nuclei. Note that the subscript 1 is omitted from  $r_1$  in the Sec. II for simplicity. The hyperfine structure of the  $^3\Delta_1$  state only was taken into account in the present study. Provided that the *electronic* matrix elements are known, the matrix elements of  $\hat{H}_{\text{hfs}}$  between states in basis set (15) can be calculated with the help of the angular momentum algebra [11]. The required electronic matrix elements are

$$A_{\parallel}^F = g_F \langle \Psi_{^3\Delta_1} | \sum_i \left( \frac{\boldsymbol{\alpha}_i \times \mathbf{r}_{2i}}{r_{2i}^3} \right)_{\zeta} | \Psi_{^3\Delta_1} \rangle, \quad (20)$$

$$A_{\parallel}^{\text{Hf}} = g_{\text{Hf}} \langle \Psi_{^3\Delta_1} | \sum_i \left( \frac{\boldsymbol{\alpha}_i \times \mathbf{r}_{1i}}{r_{1i}^3} \right)_{\zeta} | \Psi_{^3\Delta_1} \rangle, \quad (21)$$

$$eQq_0 = 2eQ \langle \Psi_{^3\Delta_1} | \sum_i \sqrt{\frac{2\pi}{5}} \frac{Y_{20}(\theta_{1i}, \phi_{1i})}{r_{1i}^3} | \Psi_{^3\Delta_1} \rangle, \quad (22)$$

$$eQq_2 = 2\sqrt{6}eQ \langle \Psi_{^3\Delta_1} | \sum_i \sqrt{\frac{2\pi}{5}} \frac{Y_{22}(\theta_{1i}, \phi_{1i})}{r_{1i}^3} | \Psi_{^3\Delta_1} \rangle, \quad (23)$$

where  $Q = 2 \langle U_{I^1, I^1}^{\text{Hf}} | \hat{Q}_0^2(I^1) | U_{I^1, I^1}^{\text{Hf}} \rangle$  is the quadrupole moment for the  $^{177,179}\text{Hf}$  nuclei. For the  $^{177}\text{Hf}$  and  $^{179}\text{Hf}$  isotopes  $I^1 = 7/2$ ,  $g_{\text{Hf}} = 0.2267$ ,  $Q = 3.365$  b and  $I^1 = 9/2$ ,  $g_{\text{Hf}} = -0.1424$ ,  $Q = 3.793$  b, respectively. The magnetic dipole hyperfine structure constant  $A_{\parallel}^F = -62.0$  MHz was measured in Ref. [1]. The magnetic dipole hyperfine structure constants  $A_{\parallel}^{\text{Hf}} = -1429$  MHz and  $A_{\parallel}^{\text{Hf}} = 898$  MHz for  $^{177}\text{Hf}^{19}\text{F}^+$  and  $^{179}\text{Hf}^{19}\text{F}^+$ , respectively, were calculated in Ref. [15]. The electric quadrupole hyperfine structure constants  $eQq_0 = -2100$  MHz,  $eQq_2 = 110$  MHz and  $eQq_0 = -2400$  MHz,  $eQq_2 = 125$  MHz for  $^{177}\text{Hf}^{19}\text{F}^+$  and  $^{179}\text{Hf}^{19}\text{F}^+$ , respectively, were calculated in the present work. The ratios for the magnetic dipole and electric quadrupole hyperfine structure constants correspond to the ratios for the nuclear g-factors and the quadrupole moments of the  $^{177}\text{Hf}$  and  $^{179}\text{Hf}$  nuclei.

#### IV. EVALUATION OF THE $eQq_0$ and $eQq_2$ CONSTANTS

To compute  $eQq_0$  in the  $^3\Delta_1$  state of HfF<sup>+</sup> we have performed relativistic coupled cluster calculations within the Dirac-Coulomb Hamiltonian using the DIRAC12 code [16]. In all the calculations the Hf-F internuclear distance in the  $^3\Delta_1$  state was set to  $3.41 a_0$  [8]. In the main calculation all 80 electrons of HfF<sup>+</sup> were included in the correlation treatment within the coupled cluster calculations with single, double, and perturbative triple amplitudes, CCSD(T), using the uncontracted Dyal CVTZ basis set for Hf [17,18] and the ccpVTZ basis set [19,20] for F. We have also applied the correction on the basis set expansion up to the uncontracted Dyal AEQZ basis set for Hf [17,18] and the aug-ccpVQZ [19,20] for F. In the calculation  $1s$ - $3d$  core electrons of Hf were excluded from the correlation treatment within the CCSD(T) method. Accounting for the perturbative triple cluster amplitudes contributes  $\approx 88$  MHz in  $eQq_0(^{177}\text{HfF}^+)$ . The contributions of the higher cluster amplitudes were estimated

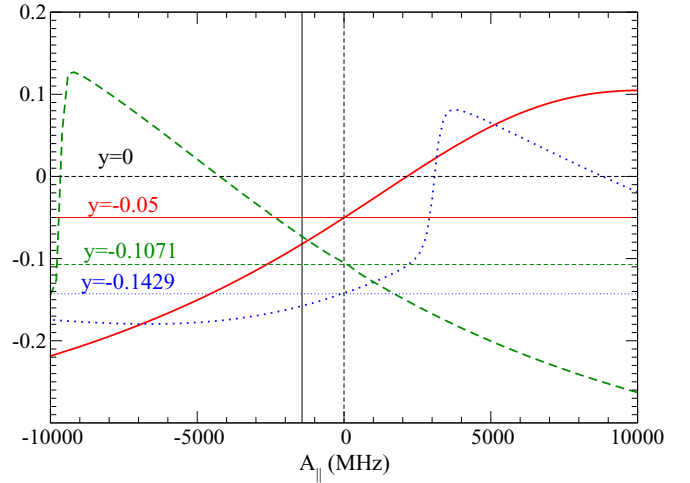


FIG. 1. Calculated MQM energy shifts (in units of  $MW_M$ ) for  $J = 1$ ,  $H^3\Delta_1$   $^{177,179}\text{Hf}^{19}\text{F}^+$  as functions of  $A_{\parallel}^{\text{Hf}}$ . Thick solid red, thick dashed green, and thick dotted blue lines correspond to  $F_1 = 9/2$ ,  $F_1 = 7/2$ , and  $F_1 = 5/2$ , respectively. Horizontal thin solid red, thin dashed green, and thin dotted blue lines correspond to values obtained by Eq. (10). Vertical black lines correspond to the values  $A_{\parallel}^{\text{Hf}} = 0$  and  $A_{\parallel}^{\text{Hf}} = -1429$  MHz obtained in calculations.  $E = 20$  V/cm,  $eQq_0 = 0$ , and  $eQq_2 = 0$  in calculations.

within the two-step approach [7,21–25], similarly to Refs. [6] and [26–29], and found to be negligible in the present case.

As follows from Eq. (23),  $eQq_2$  has no nonzero matrix elements within a main nonrelativistic term  $^3\Delta_1$ . The main contribution to  $eQq_2$  is due to the spin-orbit admixture of the  $\Pi$  state with the leading configuration  $|5s5d_{\pi}\rangle$  composed of  $5s$  and  $5d$  atomic orbitals of Hf. Then one can obtain

$$eQq_2 = 483wQ \langle 1/r^3 \rangle_{5d} \text{ MHz}, \quad (24)$$

where  $w$  is the weight of the admixture of the  $\Pi$  state,  $Q$  is the quadrupole moment of  $^{177,179}\text{Hf}$  (in barns), and  $\langle 1/r^3 \rangle_{5d} = 4.86$  a.u. as obtained from the Hartree-Fock-Dirac calculations for Hf<sup>+</sup>. The value of  $w$  can be estimated from the sensitivity to it of the body fixed g-factor

$$G_{\parallel} = \frac{1}{\Omega} \langle ^3\Delta_1 | \hat{L}_n^e - g_S \hat{S}_n^e | ^3\Delta_1 \rangle \approx 2 - 2.002319 + w, \quad (25)$$

where  $g_S = -2.002319$  is the free-electron g-factor. The same approximation as for Eq. (24) was used in Eq. (25). Then using the experimental value  $G_{\parallel} = 0.011768$  [14,30] one obtains, at  $w = 0.014$ ,  $eQq_2 = 110$  MHz and  $eQq_2 = 125$  MHz for  $^{177}\text{Hf}^{19}\text{F}^+$  and  $^{179}\text{Hf}^{19}\text{F}^+$ , respectively.

#### V. RESULTS AND DISCUSSION

In Figs. 1–3 results for MQM shifts as functions of  $A_{\parallel}^{\text{Hf}}$ ,  $eQq_0$ , and  $eQq_2$  are shown for  $^{177}\text{Hf}^{19}\text{F}^+$ . One can see that the MQM shift strongly depends on  $eQq_2$  and decreases as  $eQq_2$  increases. Similar dependencies are seen for the SP and  $e$ EDM shifts. The reason is that the electric quadrupole hyperfine interaction causes the sublevels  $\Omega = +1$  and  $\Omega = -1$ , which have different signs for  $T$ ,  $P$ -odd shifts, to mix. The coupling of states with different signs of  $\Omega$  is proportional

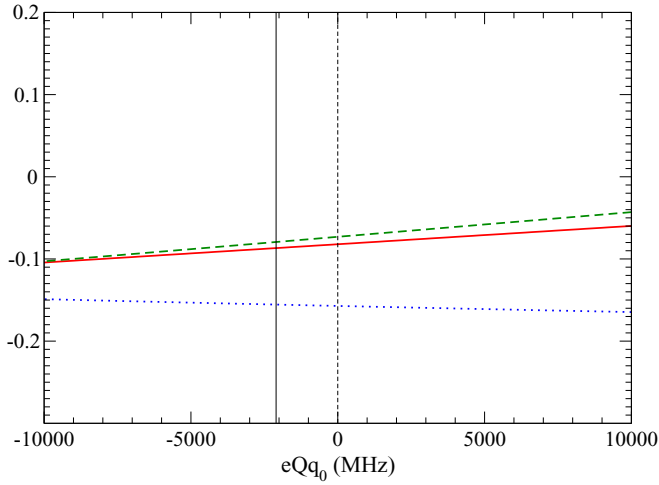


FIG. 2. Calculated MQM energy shifts (in units of  $MW_M$ ) for  $J = 1$ ,  $H^3\Delta_1$   $^{177}\text{Hf}^{19}\text{F}^+$  as functions of  $eQq_0$ . Solid red, dashed green, and dotted blue lines correspond to  $F_1 = 9/2$ ,  $F_1 = 7/2$ , and  $F_1 = 5/2$ , respectively. Vertical black lines correspond to the values  $eQq_0 = 0$  and  $eQq_0 = -2100$  MHz obtained in calculations.  $E = 20$  V/cm,  $A_{\parallel}^{\text{Hf}} = -1429$  MHz, and  $eQq_2 = 0$  in calculations.

to  $eQq_2$  as follows from Eq. (23). The least dependence is observed for the  $eQq_0$  constant. Hamiltonians (6) and (7) do not mix different rotational levels and therefore are almost independent of the  $A_{\parallel}^{\text{Hf}}$  and  $eQq_0$  constants. In Table I the calculated  $T$ ,  $P$ -odd shifts accounting for the hyperfine and Stark interactions between different rotational levels compared with those obtained from Eqs. (8)–(10) are listed. The values are quite different and the former demonstrate a large dependence on the electric field.

For completely polarized  $\text{HfF}^+$  the  $e\text{EDM}$  and  $\text{SP}$  interaction energy shifts approach the  $d_e E_{\text{eff}}^a$  and  $k_{\text{SP}} W_{\text{SP}}$  values, respectively, which are independent of the  $F_1$  quantum number. As is evident from Table I the MQM shifts depend on  $F_1$ . This fact must be used to distinguish the MQM from

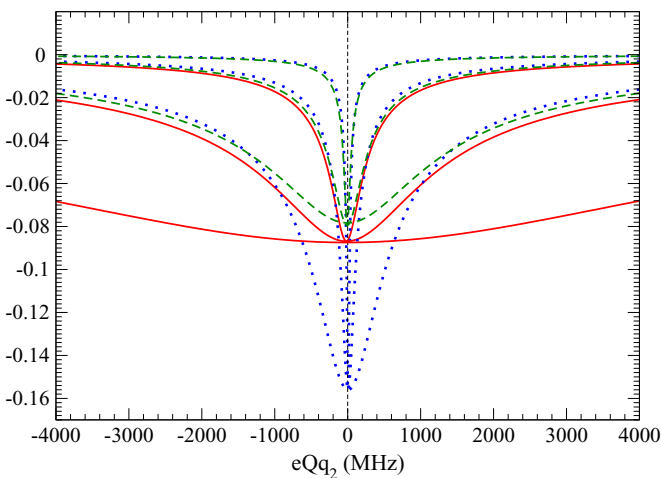


FIG. 3. Calculated MQM energy shifts (in units of  $MW_M$ ) for  $J = 1$ ,  $H^3\Delta_1$   $^{177}\text{Hf}^{19}\text{F}^+$  as functions of  $eQq_2$ . Solid red, dashed green, and dotted (blue) lines correspond to  $F_1 = 9/2$ ,  $F_1 = 7/2$ , and  $F_1 = 5/2$ , respectively.  $E = 4, 20$ , and  $100$  V/cm,  $A_{\parallel}^{\text{Hf}} = -1429$  MHz, and  $eQq_0 = -2100$  MHz in calculations.

TABLE I.  $\delta_M$ ,  $\delta_d$ , and  $\delta_{\text{SP}}$  shifts (in units of  $MW_M$ ,  $d_e E_{\text{eff}}^a$ , and  $k_{\text{SP}} W_{\text{SP}}$ , respectively) for  $J = 1$ ,  $H^3\Delta_1$ . Numerical calculations take into account interaction between different rotational levels.

$F_1$	Electric		$\delta_M$		$\delta_d$ ( $\delta_{\text{SP}}$ ):	
	field (V/cm)	Eq. (10) <sup>b</sup>	Numerical calculation	numerical calculation <sup>c</sup>		
$^{177}\text{Hf}^{19}\text{F}^+$						
9/2	4	0.05000	0.07879	0.90804		
	20		0.08651	0.99577		
	100		0.08742	0.99983		
7/2	4	0.14286	0.02278	0.14581		
	20		0.09268	0.59325		
	100		0.15050	0.96511		
5/2	4	0.10714	0.02864	0.36015		
	20		0.07048	0.88791		
	100		0.07789	0.99466		
$^{179}\text{Hf}^{19}\text{F}^+$						
11/2	4	0.05000	0.02165	0.72080		
	20		0.02961	0.98200		
	100		0.03074	0.99926		
9/2	4	0.13333	0.00446	0.03696		
	20		0.02195	0.18187		
	100		0.08213	0.67962		
7/2	4	0.09167	0.06467	0.53716		
	20		0.11499	0.95405		
	100		0.12101	0.99803		

<sup>a</sup> $\delta_d$  and  $\delta_{\text{SP}}$  are equal.

<sup>b</sup>Values obtained using Eq. (10) are independent of the values of the electric field.

<sup>c</sup>If the hyperfine interaction with the hafnium nucleus is not taken into account (or we consider the  $^{180}\text{Hf}^{19}\text{F}^+$  ion where it is identically 0), then the  $\delta_d$  and  $\delta_{\text{SP}}$  shifts are equal to unity for the fields used in the table.

the scalar  $T$ ,  $P$ -odd effects. Equation (10) gives a difference of approximately a factor of 3 between the largest and the smallest shifts for both  $^{177}\text{Hf}^{19}\text{F}^+$  and  $^{179}\text{Hf}^{19}\text{F}^+$  ions. One can see in Table I that more accurate numerical calculations give factors of approximately 2 and 4 for  $^{177}\text{Hf}^{19}\text{F}^+$  and  $^{179}\text{Hf}^{19}\text{F}^+$ , respectively. The MQM can be expressed in terms of the proton and neutron EDMs  $d_p$  and  $d_n$ , QCD vacuum angle  $\theta$ , and quark chromo-EDMs  $\tilde{d}_u$  and  $\tilde{d}_d$ . Using these data [3], the calculated value  $W_M = 0.494 \frac{10^{33} \text{ Hz}}{e \text{ cm}^2}$  [26], and data in Table I, one obtains that the current limits  $|d_p| < 2.0 \times 10^{-25} e \text{ cm}$ ,  $|\theta| < 1.5 \times 10^{-10}$ , and  $|\tilde{d}_u - \tilde{d}_d| < 5.7 \times 10^{-27} e \text{ cm}$  correspond to energy shifts of less than 6, 8, and 18  $\mu\text{Hz}$  for  $^{177}\text{Hf}^{19}\text{F}^+$  and less than 3, 5, and 11  $\mu\text{Hz}$  for  $^{179}\text{Hf}^{19}\text{F}^+$ , respectively.

## VI. CONCLUSION

We have calculated the  $T$ ,  $P$ -odd energy shifts produced by MQM,  $e\text{EDM}$ , and  $\text{SP}$  interactions for the ground rotational  $J = 1$  hyperfine levels of the  $^3\Delta_1$  electronic state of  $^{177}\text{Hf}^{19}\text{F}^+$  and  $^{179}\text{Hf}^{19}\text{F}^+$  ions. It is found that taking into account the hyperfine interaction is critically important for accurate evaluation of the effects. The MQM shifts depend on a hyperfine sublevel of the  $J = 1$  rotational state.

We found that there is a difference of a factor of 2 and 4 between the largest and the smallest shifts for  $^{177}Hf^{19}F^+$  and  $^{179}Hf^{19}F^+$ , respectively. The experiment on  $^{177}Hf^{19}F^+$  and  $^{179}Hf^{19}F^+$ , similarly to the one on  $^{180}Hf^{19}F^+$  [1], can be performed using rotating electric and magnetic fields which trap the cation. We have shown that  $^{177}Hf^{19}F^+$  and  $^{179}Hf^{19}F^+$  require an electric field much larger than that of  $^{180}Hf^{19}F^+$  to be polarized. However, our calculations have shown that the  $F_1 = 9/2, 5/2$  and  $F_1 = 11/2, 7/2$  states of  $^{177}Hf^{19}F^+$  and  $^{179}Hf^{19}F^+$ , respectively, for the electric field  $\sim 20$  V/cm used in the experiment [1], are almost completely polarized.

## ACKNOWLEDGMENTS

The formulation of the problem and the molecular calculations were supported by Russian Science Foundation Grant No. 18-12-00227. The electronic structure calculations of the  $eQq_0$  parameter were supported by RFBR, under research Project No. 16-32-60013 mol\_a\_dk. Electronic structure calculations were performed at the PIK data center of NRC Kurchatov Institute—PNPI. The calculations of the nuclear structure were supported by the Australian Research Council Grant No. DP150101405, Gutenberg Fellowship and New Zealand Institute for Advanced Studies.

- 
- [1] W. B. Cairncross, D. N. Gresh, M. Grau, K. C. Cossel, T. S. Roussy, Y. Ni, Y. Zhou, J. Ye, and E. A. Cornell, *Phys. Rev. Lett.* **119**, 153001 (2017).
- [2] A. N. Petrov, *Phys. Rev. A* **97**, 052504 (2018).
- [3] V. V. Flambaum, D. DeMille, and M. G. Kozlov, *Phys. Rev. Lett.* **113**, 103003 (2014).
- [4] L. V. Skripnikov, A. N. Petrov, A. V. Titov, and V. V. Flambaum, *Phys. Rev. Lett.* **113**, 263006 (2014).
- [5] J. Ye (private communication).
- [6] L. V. Skripnikov, A. N. Petrov, N. S. Mosyagin, A. V. Titov, and V. V. Flambaum, *Phys. Rev. A* **92**, 012521 (2015).
- [7] L. V. Skripnikov and A. V. Titov, *Phys. Rev. A* **91**, 042504 (2015).
- [8] K. C. Cossel, D. N. Gresh, L. C. Sinclair, T. Coffey, L. V. Skripnikov, A. N. Petrov, N. S. Mosyagin, A. V. Titov, R. W. Field, E. R. Meyer *et al.*, *Chem. Phys. Lett.* **546**, 1 (2012).
- [9] M. G. Kozlov, V. I. Fomichev, Yu. Yu. Dmitriev, L. N. Labzovsky, and A. V. Titov, *J. Phys. B* **20**, 4939 (1987).
- [10] L. R. Hunter, *Science* **252**, 73 (1991).
- [11] L. D. Landau and E. M. Lifshitz, *Quantum Mechanics*, 3rd ed. (Pergamon, Oxford, UK, 1977).
- [12] A. N. Petrov, *Phys. Rev. A* **83**, 024502 (2011).
- [13] A. N. Petrov, L. V. Skripnikov, A. V. Titov, N. R. Hutzler, P. W. Hess, B. R. O’Leary, B. Spaun, D. DeMille, G. Gabrielse, and J. M. Doyle, *Phys. Rev. A* **89**, 062505 (2014).
- [14] A. N. Petrov, L. V. Skripnikov, and A. V. Titov, *Phys. Rev. A* **96**, 022508 (2017).
- [15] L. V. Skripnikov, *J. Chem. Phys.* **147**, 021101 (2017).
- [16] H. J. Aa. Jensen, R. Bast, T. Saue, and L. Visscher, with contributions from V. Bakken, K. G. Dyall, S. Dubillard, U. Ekström, E. Eliav, T. Enevoldsen, T. Fleig, O. Fossgaard, A. S. P. Gomes, T. Helgaker, J. K. Lærdahl, Y. S. Lee, J. Henriksson, M. Iliaš, Ch. R. Jacob, S. Knecht, S. Komorovský, O. Kullie, C. V. Larsen, H. S. Nataraj, P. Norman, G. Olejniczak, J. Olsen, Y. C. Park, J. K. Pedersen, M. Pernpointner, K. Ruud, P. Sałek, B. Schimmelpfennig, J. Sikkema, A. J. Thorvaldsen, J. Thyssen, J. van Stralen, S. Villaume, O. Visser, T. Winther, and S. Yamamoto, DIRAC, a relativistic ab initio electronic structure program, Release DIRAC12 (2012); <http://www.diracprogram.org>.
- [17] K. G. Dyall, *Theor. Chem. Acc.* **117**, 491 (2006).
- [18] K. G. Dyall, *Theor. Chem. Acc.* **131**, 1217 (2012).
- [19] T. H. Dunning Jr., *J. Chem. Phys.* **90**, 1007 (1989).
- [20] R. A. Kendall, T. H. Dunning Jr., and R. J. Harrison, *J. Chem. Phys.* **96**, 6796 (1992).
- [21] A. N. Petrov, N. S. Mosyagin, T. A. Isaev, A. V. Titov, V. F. Ezhov, E. Eliav, and U. Kaldor, *Phys. Rev. Lett.* **88**, 073001 (2002).
- [22] A. V. Titov, N. S. Mosyagin, A. N. Petrov, T. A. Isaev, and D. P. DeMille, *Progr. Theor. Chem. Phys.* **15**, 253 (2006).
- [23] L. V. Skripnikov, A. V. Titov, A. N. Petrov, N. S. Mosyagin, and O. P. Sushkov, *Phys. Rev. A* **84**, 022505 (2011).
- [24] N. S. Mosyagin, A. V. Zaitsevskii, L. V. Skripnikov, and A. V. Titov, *Int. J. Quantum Chem.* **116**, 301 (2016).
- [25] L. V. Skripnikov and A. V. Titov, *J. Chem. Phys.* **145**, 054115 (2016).
- [26] L. V. Skripnikov, A. V. Titov, and V. V. Flambaum, *Phys. Rev. A* **95**, 022512 (2017).
- [27] L. V. Skripnikov, D. E. Maison, and N. S. Mosyagin, *Phys. Rev. A* **95**, 022507 (2017).
- [28] L. V. Skripnikov, *J. Chem. Phys.* **145**, 214301 (2016).
- [29] L. V. Skripnikov and A. V. Titov, *J. Chem. Phys.* **142**, 024301 (2015).
- [30] H. Loh, K. C. Cossel, M. C. Grau, K.-K. Ni, E. R. Meyer, J. L. Bohn, J. Ye, and E. A. Cornell, *Science* **342**, 1220 (2013).